Neurobiology of Disease

Human Tobacco Smokers in Early Abstinence Have Higher Levels of β_2*Nicotinic Acetylcholine Receptors than Nonsmokers

Julie K. Staley,[1,3] Suchitra Krishnan-Sarin,[1] Kelly P. Cosgrove,[1,3] Erica Krantzler,[1,3] Erin Frohlich,[1,3] Edward Perry,[1,3] Joel A. Dubin,[1] Kristina Estok,[1,3] Eric Brenner,[1,3] Ronald M. Baldwin,[1,3] Gilles D. Tamagnan,[1,3,4] John P. Seibyl,[1,4] Peter Jatlow,[1,2] Marina R. Picciotto,[1] Edythe D. London,[5] Stephanie O'Malley,[1] and Christopher H. van Dyck[1]

Departments of [1]Psychiatry and [2]Laboratory Medicine, Yale University School of Medicine, New Haven, Connecticut 06511, [3]Veterans Administration Connecticut Healthcare System, West Haven, Connecticut 06516, [4]Institute for Neurodegenerative Disorders, New Haven, Connecticut 06510, and [5]Departments of Psychiatry and Biobehavioral Sciences, and Molecular and Medical Pharmacology, David Geffen School of Medicine, University of California, Los Angeles, Los Angeles, California 90024

Nicotine, the addictive chemical in tobacco smoke, initiates its actions in brain through nicotinic acetylcholine receptors (nAChRs). In particular, nAChRs containing β_2-subunits (β_2*-nAChRs) the most prevalent subtype, mediate the reinforcing properties of nicotine. We hypothesized that abnormal numbers of β_2*-nAChRs during early abstinence contribute to the perpetuation of addiction to tobacco smoking. Using molecular imaging, specifically single-photon emission computed tomography with the nAChR agonist radiotracer [^{123}I]5-IA-85380 ([^{123}I]5-IA), we imaged β_2*-nAChR availability in human smokers. First, using nonhuman primates treated chronically with nicotine, we estimated the time interval necessary for smokers to abstain from smoking so that residual nicotine would not interfere with [^{123}I]5-IA binding to the β_2*-nAChR as ~7 d. Thus, we imaged human smokers at 6.8 ± 1.9 d (mean ± SD) of abstinence. Abstinence was confirmed by daily assessments of urinary cotinine and expired carbon monoxide levels. In smokers, [^{123}I]5-IA uptake was significantly higher throughout the cerebral cortex (26–36%) and in the striatum (27%) than in nonsmokers, suggesting higher β_2*-nAChR in recently abstinent smokers. β_2*-nAChR availability in recently abstinent smokers correlated with the days since last cigarette and the urge to smoke to relieve withdrawal symptoms but not the severity of nicotine dependence, severity of nicotine withdrawal, or the desire to smoke. Higher brain β_2*-nAChR during early abstinence indicates that, when smokers quit smoking, they do so in the face of a significant increase in the receptors normally activated by nicotine. Greater β_2*-nAChR availability during early abstinence may impact the ability of smokers to maintain abstinence.

Key words: **brain; nicotine; nicotinic acetylcholine receptor; human; smokers; addiction; thalamus**

Introduction

Despite the well known health risks of tobacco smoking, 24.9% of the United States population continues to smoke (Grant et al., 2004). Although tobacco smoke contains >4000 chemicals, its addictive properties have been attributed primarily to nicotine. In brain, nicotine acts via nicotinic acetylcholine receptors (nAChRs) to initiate a cascade of neurochemical reactions that includes the release of almost every major neurotransmitter and widespread activation of most neuronal networks. Adaptations of nAChRs in response to repeated and protracted nicotine exposure likely contribute to the addiction to cigarette smoking.

Postmortem studies of human brain have suggested that numbers of nAChRs are higher in smokers than in nonsmokers or former smokers (Benwell et al., 1988; Breese et al., 1997; Perry et al., 1999), and animals exposed to nicotine chronically exhibit increased levels of nAChRs in the brain (Marks et al., 1983, 1985, 1992; Schwartz and Kellar, 1983). Because the reinforcing properties of nicotine have been linked specifically to nAChRs that contain the β_2 subunit (β_2*-nAChRs) (Picciotto et al., 1998), an understanding of the adaptive changes in β_2*-nAChR number during acute abstinence and their relationship to behavioral correlates of tobacco smoking may advance the development of improved pharmacotherapies to aid smoking cessation. With the recent development of [^{123}I]5-IA-85380 ([^{123}I]5-IA), a radioligand that has specificity for the agonist binding site on β_2*-nAChRs (Musachio et al., 1998, 1999; Horti et al., 1999), it is now possible to measure this site in living smokers during acute abstinence from smoking and to determine the relationship of brain

Received Feb. 6, 2006; revised June 16, 2006; accepted July 5, 2006.

This work was supported by National Institutes of Health Grants R01DA015577, K01 AA00288 (J.K.S.), P50 DA 13334, P50 AA15632 (S.O.M.), and K02DA00436 (M.R.P.), Mental Illness Research, Education, and Clinical Centers, and The Robert Leet and Clara Guthri Patterson Trust. We thank Eileen Smith, Gina Morano, Andrea Perez, Stacey Ross, Jane Bartosik, Louis Amici, Nina Sheung, Mohammed Al Tikriti, and Shawna Ellis for technical support.

Correspondence should be addressed to Dr. Julie K. Staley, Department of Psychiatry, Yale University and Veterans Administration Connecticut Hospital System 116A2, 950 Campbell Avenue, West Haven, CT 06516. E-mail: julie.staley@yale.edu.

DOI:10.1523/JNEUROSCI.0546-06.2006

 0270-6474/06/268707-08$15.00/0

β_2*-nAChR availability to smoking behavior and nicotine withdrawal symptoms.

The goals of this study were to image β_2*-nAChRs in living human smokers using [^{123}I]5-IA single-photon emission computed tomography (SPECT) and to compare receptor availability in smokers during early abstinence with corresponding values in nonsmokers. We hypothesized that β_2*-nAChR availability would be higher in recently abstinent smokers than in nonsmokers. Because nicotine competes with [^{123}I]5-IA binding for binding to nAChRs (Mukhin et al., 2000), we first studied nonhuman primates chronically treated with nicotine to estimate the time interval necessary for smokers to abstain from smoking (before [^{123}I]5-IA SPECT imaging) to ensure that residual nicotine or metabolite would not interfere with radioligand binding to the receptor.

Materials and Methods

Nonhuman primates. Two gonadally intact adolescent (4–5 years old) male rhesus monkeys (*Macacca mulatta*, 8.9 and 7.7 kg) participated in the studies. Monkeys were housed individually in temperature- and humidity-controlled rooms maintained on a 12 h light/dark schedule with lights on at 7:00 A.M. Monkeys were fed Monkey Diet Biscuit daily after each experimental session and were weighed biweekly. They participated in a psychological enrichment program. The animal protocol was approved by the Yale and Veterans Administration Animal Care and Use Committees and is in compliance with United States Public Health Service Policy on Humane Care and Use of Laboratory Animals.

Nicotine administration. Nicotine was administered orally using the dose escalation paradigm described previously (Pietila et al., 1998). Nicotine (Sigma, St. Louis, MO) was administered in a saccharin–Kool-Aid (Kraft Foods, Northfield, IL) solution as the sole source of fluid on a daily basis (with the exception of days of nicotine withdrawal before each scan and also for the day of and immediately after the scan). During weeks 0–4, the animals increased their average nicotine consumption from 3.3 to 37.5 mg/kg. During the last 5–8 weeks of the study, the animals' average daily nicotine consumption was 30–38 mg/kg. After 6 and 8 weeks, the nicotine solution was removed and the monkeys had access to water. Monkeys were imaged 1–2 d after 6 weeks and 7 d after 8 weeks of nicotine exposure.

[^{123}I]5-IA SPECT imaging of nonhuman primates. Nonhuman primates were imaged using methods described previously (Staley et al., 2000). Each animal was fasted for 18–24 h before SPECT scanning. Two hours before the study, the animal was immobilized using ketamine (10 mg/kg, i.m.), positioned on the bed of the SPECT camera, and immediately prepared with an endotracheal tube for administration of 2.5% isoflurane. Glycopyrrolate (10 μg/kg, i.m.), a long-acting peripheral anticholinergic drug that does not cross the blood–brain barrier, was coadministered with the initial ketamine injection to decrease respiratory and digestive secretions. Body temperature was maintained at 35–36°C using a heated water blanket. Vital signs, including heart rate, respiration rate, oxygen saturation, and body temperature, were monitored every 15–30 min throughout each study. An intravenous perfusion line with 0.9% saline was placed and used for the bolus injection and infusion of the radiotracer. A second line was placed and was maintained with lactated Ringer's solution at a rate of 1.8 ml $\cdot$ kg^{-1} $\cdot$ h^{-1} throughout the experiment and was used to obtain blood samples. The animal's head was immobilized within the gantry with a "bean bag" that hardens on evacuation (Olympic Medical, Seattle, WA). [^{123}I]5-IA was prepared to give a product with radiochemical purity of >90%, and [^{123}I]5-IA plasma levels were measured as described previously (Zoghbi et al., 2001). Regional [^{123}I]5-IA uptake was assessed after administration of [^{123}I]5-IA using the bolus (40.0 ± 9.3 MBq) plus constant infusion (6.7 ± 1.9 MBq/h) paradigm. Fifteen minute SPECT scans were acquired continuously for 8 h with the nonhuman primate brain-dedicated multislice CERASPECT camera (Digital Scintigraphics, Waltham, MA), and magnetic resonance imaging (MRI) scans were obtained and processed as described previously (Staley et al., 2000). The primary outcome measure for regional brain uptake was V_T', which is proportional to the binding potential (BP) (B_{max}/K_D), assuming that there is no change in affinity (K_D) and that nondisplaceable uptake does not differ between animals and studies. Percentage change was calculated for each region of interest (ROI) by the formula [((V_T' during study condition/V_T' during baseline) − 1) * 100] at equilibrium. Equilibrium was established by hour 4 after injection of the radiotracer, as demonstrated by stable levels of regional [^{123}I]5-IA uptake with average changes of 0.43%/h for cortical regions and 0.62%/h for subcortical areas.

Measurement of plasma and urine cotinine levels. On each scan day, plasma cotinine and nicotine concentrations were measured in plasma obtained from EDTA anti-coagulated blood samples obtained at the start and the completion of the [^{123}I]5-IA SPECT scan. Samples were centrifuged at room temperature and promptly frozen. Samples were stored in the laboratory, protected from light at −60–70°F. Cotinine and nicotine concentrations in serum were assayed using reversed-phase HPLC. The procedure was modified (Hariharan and VanNoord, 1988) by substitution of an aqueous micro-back-extraction clean-up step in place of solvent evaporation. After addition of an internal standard (2-phenylimidazole), cotinine and nicotine were extracted from alkalinized serum with a 40:60 mixture of dichloromethane/hexane. After a micro-back extraction into 0.1 M H_3PO_4, the aqueous phase was chromatographed on a C6 reversed-phase column using a mobile phase of 10% acetonitrile buffered to pH 4.8 and containing 20 ml of triethylamine and 0.6 g/L octane-sulfonic acid. Between-day coefficients of variation for nicotine, at concentrations of 4, 20, and 40 ng/ml were 17.7, 6.2, and 2.9%, respectively. For cotinine, at concentrations of 20 and 200 ng/L, they were 11.6 and 6.6%, respectively. Plasma cotinine levels in the nonhuman primates were within the range of plasma cotinine levels in human tobacco smokers (>15 ng/ml, 1 pack per day; >300 ng/ml, >25 cigarettes per day). Technical problems precluded determining plasma levels in one monkey at 6 weeks/2 d withdrawal.

Urinary cotinine levels were monitored daily during the 7 d nicotine withdrawal period using Accutest NicoMeter cotinine test strips (Jant Pharmacal, Encino, CA).

Human subjects. Smokers (n = 16) and nonsmokers (n = 16) were recruited from the Yale–New Haven Medical Center, Connecticut Mental Health Center, Yale University, the West Haven Veterans Administration Connecticut Hospital System, or the community by word of mouth, posters, or newspaper advertisement. All subjects signed informed consent, as approved by the Yale University School of Medicine Human Investigation Committee, and the West Haven Veterans Administration Human Subjects Subcommittee, for relevant procedures conducted at each site. All smokers and nonsmokers were evaluated by physical examination, electrocardiogram, routine laboratory screening of both blood and urine, and structured interviews using the Structured Clinical Interview of Diagnostic and Statistical Manual of Mental Disorders (DSM) to rule out psychopathology or presence of psychiatric disorders based on DSM IV criteria.

All subjects met the following criteria: (1) 18–60 years of age; (2) able to read and write English; (3) alcohol consumption, by men, <21 alcohol drinks per week and less than five alcohol drinks per occasion and, by women, <14 alcohol drinks per week and less than four alcohol drinks per occasion; (4) no evidence of acute or unstable medical or neurological illness; (5) no evidence of atrioventricular heart block greater than the first degree, evidence of ischemia, and, any unstable cardiac rhythm; (6) no hypertension defined as sitting systolic blood pressure of >160 mmHg and/or sitting diastolic blood pressure of >100 mmHg; (7) sitting pulse rate <100 beats per minute; (8) no axis I diagnosis other than nicotine dependence; (9) no current or past year criteria for abuse or dependence on cocaine, marijuana, opiates, or alcohol; (10) no regular use of any psychotropic drugs, including anxiolytics and antidepressants and herbal products within the past 6 months; (11) never used ecstasy (3,4-methylenedioxymethamphetamine); (12) not pregnant or nursing; and (13) no pacemaker or metal in body that would preclude safety of an MRI scan. Smokers had to meet the following additional criteria: (1) smoke ≥10 cigarettes per d for at least 1 year; (2) carbon monoxide levels ≥8 ppm; and (3) plasma cotinine levels ≥150 ng/ml. Nonsmokers were recruited to match the smokers on the basis of age, sex, and race and met

the following additional criteria: (1) smoked <100 cigarettes in lifetime; (and 2) plasma cotinine levels <15 ng/ml. In addition, women nonsmokers were matched to women smokers based on menstrual cycle phase. On the SPECT scan day, menstrual cycle phase was documented by self-report of the first day of the last menses and was categorized as follicular (days 1–13) or luteal (days 15–28) for the purpose of matching smokers and nonsmokers. Self-reports of menstrual cycle phase were validated by plasma estrogen and progesterone levels.

The severity of nicotine dependence was assessed using the Fagerström Test for Nicotine Dependence (FTND) (Heatherton et al., 1991), nicotine withdrawal symptoms were assessed using the Minnesota Withdrawal Questionnaire (MWQ) (Hatsukami et al., 1984), and the urge to smoke (or craving) was assessed using the Urge to Smoke Questionnaire (Tiffany and Drobes, 1991).

Smoking cessation: contingency management. Smokers (12 of 16) were assisted in quitting smoking using brief behavioral counseling based on Clinical Practice Guidelines and contingency management (Stitzer and Bigelow, 1985; Stitzer et al., 1986; Roll et al., 1996). Four smokers abstained without daily contingency management. Urine cotinine concentrations were monitored using the semiquantitative Accutest NicoMeter Cotinine Test.

[^{123}I]5-IA SPECT imaging of human subjects. Human smokers were imaged as described previously (Staley et al., 2005). In brief, [^{123}I]5-IA was administered using the bolus plus constant infusion paradigm with a bolus to infusion ratio of 7.0 h, an average bolus of 135 ± 13 and 129 ± 20 MBq, and infusion rates of 214 ± 3 and 212 ± 3 MBq/h for the 16 nonsmokers and 16 smokers, respectively. Three SPECT scans (30 min each) were obtained between 6 and 8 h of infusion, and plasma samples were collected immediately before and after the scan to quantify total parent and the free fraction of parent tracer in plasma (f_1, free fraction) (Zoghbi et al., 2001).

Image analysis. SPECT emission images were filtered using a three-dimensional (3D) Butterworth filter (order, 10; cutoff frequency, 0.24 cycles/pixel) and reconstructed using a filtered back-projection algorithm with a ramp filter on a 128 × 128 matrix to obtain 50 slices with a pixel size of 2.06 × 2.06 × 3.56 mm in the *x*-, *y*-, and *z*-axes. Nonuniform attenuation correction was performed (Rajeevan et al., 1998). Each subject's MRI was coregistered to their SPECT image using SPM2 (Wellcome Department of Cognitive Neurology, University College London, London, UK). The coregistered MRI was used to guide the placement of standard two-dimensional ROI templates for each individual subject. A 3D volume of interest was generated for each region and transferred to the coregistered SPECT image to determine regional radioactive densities (counts per minute/pixel). Standard-sized two-dimensional regions of interest were placed on right and left hemispheres for frontal, parietal, anterior cingulate, temporoinsular, and occipital cortices, caudate and putamen, thalamus, and cerebellum. Regional β_2*-nAChR availability was determined by V_T' (regional activity/total plasma parent), a highly reproducible outcome measure (Staley et al., 2005). Two raters conducted the region of interest analyses. The interclass coefficient to assess inter-rater reliability (Rousson et al., 2002) ranged between 0.82 and 0.97 for the V_T' measure across the eight brain regions. The mean of the analyses from the two raters is reported.

A voxel-based analysis was conducted using statistical parametric mapping (SPM2). For each subject, a mean image was made from the three consecutive [^{123}I]5-IA emission scans and scaled to the total volume of distribution, V_T' (milliliters per cubic centimeter). The corresponding MRI (coregistered to the SPECT mean [^{123}I]5-IA V_T' image) was coregistered to the standard T_1 MRI in SPM2, and the coregistration parameters were applied to each mean [^{123}I]5-IA V_T' image. When all MRI and corresponding mean V_T' images were coregistered to the T_1 template, a mean MRI template and a mean [^{123}I]5-IA V_T' template were made from the corresponding scan for each study participant ($n = 32$). The mean MRI template was spatially normalized to the T_1 MRI template in SPM2, and the parameters were applied to the mean [^{123}I]5-IA V_T' template. Thereafter, each mean V_T' map from each subject was spatially normalized to the mean [^{123}I]5-IA SPECT V_T' template and smoothed using a Gaussian kernel of 12 × 12 × 12 mm.

Statistical analyses. Differences in plasma and brain outcome measures between smokers and nonsmokers were evaluated first using a multivariate ANOVA (MANOVA). Thereafter, univariate analyses were conducted using a one-way, unpaired Student's *t* test. Bonferroni's correction for multiple comparisons across eight brain regions indicated that *p* values <0.00625 were highly significant.

Correlations between regional brain [^{123}I]5-IA uptake (V_T') and clinical variables (including number of cigarettes smoked per day, FTND score, and MWQ score) were conducted using Pearson's correlation.

For voxel-based analyses, between-group analyses were conducted comparing nonsmokers and smokers. In the smokers, the relationship between [^{123}I]5-IA V_T' and various clinical measures of smoking behavior were explored. *T*-statistic images were thresholded to a minimum cluster size of 42 voxels calculated based on the nominal resolution, i.e., the full-width half-maximum, of a point source in water in the Picker Prism 3000XP SPECT camera. The anatomic location of the most significant voxel in clusters demonstrating statistical significance ($p < 0.001$) after corrections for multiple comparisons was determined after conversion of Montreal Neurological Institute stereotaxic coordinates to Talairach coordinates and submission of the results to Talairach Demon (Lancaster et al., 1997, 2000).

Results

To estimate the necessary abstinence interval in subsequent human studies, we imaged two male adolescent rhesus macaques twice (test–retest) with [^{123}I]5-IA SPECT before oral nicotine administration. Each animal participated in a third [^{123}I]5-IA SPECT scan after 6 weeks of nicotine administration and 1 or 2 d of withdrawal, and a fourth [^{123}I]5-IA SPECT scan after 2 additional weeks of nicotine treatment and 7 d of nicotine withdrawal.

Average regional [^{123}I]5-IA binding decreased from baseline (41–65% change) after 1–2 d withdrawal, whereas [^{123}I]5-IA binding robustly increased from baseline (240–276% change)

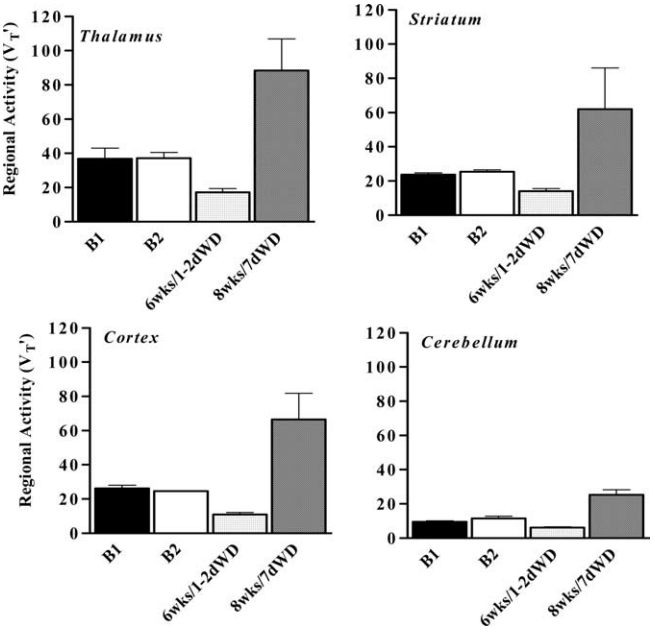

Figure 1. [^{123}I]5-IA binding to β_2-nAChRs before (at baseline; B1, B2) and after (6 and 8 weeks) unrestricted oral nicotine administration in nonhuman primates. After 6 weeks of oral nicotine administration, animals were withdrawn for 1–2 d, and, after 8 weeks of nicotine administration, animals were withdrawn for 7 d before [^{123}I]5-IA SPECT imaging. Regional [^{123}I]5-IA uptake is represented by V_T'. Note the reproducibility of measurement indicated by lack of change between B1 and B2, the profound decrease followed by 1–2 d of withdrawal (41–65% change at 6 weeks of nicotine treatment), and the dramatic increase followed by 7 d of withdrawal (>200% after 8 weeks of nicotine treatment). The cortex represents the mean values for all cortical measures. Individual cortical values and values for the thalamus, striatum, and cerebellum are detailed in Table 1.

after 7 d nicotine withdrawal (Fig. 1, Table 1). Venous plasma nicotine levels were negligible (< 5 ng/ml) on all SPECT scan days (1, 2, and 7 d of withdrawal), whereas levels of plasma cotinine (the primary metabolite of nicotine) ranged from 265 to 299 ng/ml at 1–2 d withdrawal and from 75 to 166 ng/ml at 7 d withdrawal. Daily measurements of urinary cotinine during nicotine withdrawal demonstrated levels of >10,000 ng/ml for days 1–4, with progressive decreases to <250 ng/ml at 7 d withdrawal. Decreased β_2*-nAChR availability and elevated plasma and urinary cotinine at 1–2 d withdrawal, interpreted in combination with the *in vitro* data (for review, see Esterlis et al., 2005) demonstrating greater concentrations of nAChRs within hours of the last nicotine exposure, suggest that residual nicotine or a metabolite, such as cotinine or nornicotine, blocked [^{123}I]5-IA from binding to β_2*-nAChR during the first 48 h of nicotine withdrawal. After 7 d of nicotine withdrawal, when plasma and urinary cotinine levels were significantly lower than at baseline, we observed the expected elevation in Dβ_2*-nAChR availability, suggesting that ~7 d of abstinence from smoking is needed before imaging to ensure that residual nicotine and/or its metabolite(s) did not interfere with [^{123}I]5-IA binding to β_2*-nAChR in smokers.

Next, we studied brain β_2*-nAChR availability in 16 nonsmokers (35.1 ± 12.0 years) and 16 age- and sex-matched smokers (37.0 ± 12.2 years) using [^{123}I]5-IA SPECT. Each group consisted of seven men and nine women. Women nonsmokers and smokers were also matched by phase of the menstrual cycle. Fifteen of the 16 nonsmokers had never smoked a cigarette, and one reported experimenting with smoking 18 years before study participation but did not meet criteria for past dependence. Smokers smoked at least 10 cigarettes per day for at least 1 year, with an average of 20.1 ± 7.5 cigarettes per day for 18.6 ± 10.1 years. Smoking status was confirmed by plasma cotinine levels (215.4 ± 140.4 ng/ml) and also by carbon monoxide levels in expired air (18.4 ± 9.8 ppm at intake). Smokers demonstrated average scores of 4.6 ± 3.0 on the FTND, signifying a moderate level of dependence.

Smokers abstained from smoking for 6.8 ± 1.9 d to allow time for nicotine or metabolite to clear from brain. Urine cotinine concentrations declined from day 1 (range of 1000–10,000 ng/ml cotinine) for all smokers, except one (100–250 ng/ml) to day 4 of abstinence (0–1000 ng/ml). On the SPECT scan day, urinary cotinine levels were <250 ng/ml for 14 of 16 smokers and <1000 ng/ml for two smokers. Carbon monoxide levels for smokers and nonsmokers were 3.5 ± 2.3 and 1.0 ± 2.0 ppm, respectively. Nonsmokers and smokers were administered [^{123}I]5-IA using the bolus plus constant infusion paradigm and were imaged between 6 and 8 h. The concentration of unmetabolized [^{123}I]5-IA and the percentage of [^{123}I]5-IA not bound to plasma proteins (f_1) did not vary significantly between nonsmokers and smokers [0.31 ± 0.09 and 0.26 ± 0.08 kBq/ml, respectively; 95% confidence interval (−0.114, 0.009); $p = 0.09$; and 35.4 ± 3.2 and 36.6 ± 4.9%, respectively; $p = 0.44$]. Voxel-based analyses (df = 30) demonstrated significantly higher β_2*-nAChR availability for a large cluster ($T = 5.20$; $p = 0.000$ corrected) that included the parietal cortex [Brodmann's area 40 (BA 40)], cingulate gyrus (BA 31), middle temporal gyrus (BA 39), and for two smaller clusters in the middle frontal gyrus that included BA 6 ($T = 4.43$; $p = 0.03$ corrected) and BA 9 ($T = 4.19$; $p = 0.04$ corrected) in recently abstinent smokers compared with nonsmokers (Fig. 2). MANOVA of the region of interest analyses for eight brain regions confirmed significantly higher [^{123}I]5-IA brain uptake in recently abstinent smokers compared with nonsmokers (F = 11.2821; df = 8,23; p values <0.001) in cortical areas (26–36%

Table 1. β_2*-nAChR availability in nonhuman primate brain before and after nicotine treatment

	B1	B2	6wk/1,2d	% Decrease	8wk/7d	% Increase
Thalamus	36.7 ± 6.4	37.2 ± 4.7	17.1 ± 3.3	53.7%	88.4 ± 26.0	239%
Striatum	23.7 ± 1.1	25.5 ± 1.5	14.1 ± 2.1	42.8%	61.9 ± 34.0	252%
Parietal cortex	25.8 ± 3.0	23.6 ± 0.4	9.6 ± 0.8	61.3%	68.2 ± 21.1	276%
Frontal cortex	28.4 ± 1.3	26.9 ± 0.6	9.7 ± 1.3	65.1%	73.4 ± 26.5	266%
Cingulate cortex	32.7 ± 2.3	30.4 ± 0.0	13.4 ± 1.9	57.7%	77.0 ± 27.6	244%
Temporal cortex	23.2 ± 1.6	23.7 ± 0.6	12.1 ± 2.4	48.3%	59.4 ± 20.4	254%
Occipital cortex	19.9 ± 2.7	19.8 ± 0.6	10.3 ± 1.4	48.0%	54.4 ± 13.0	274%
Cerebellum	9.6 ± 0.5	11.6 ± 1.9	6.2 ± 0.4	41.2%	25.4 ± 4.2	240%

B1, Baseline 1; B2, baseline 2; 6wk/1,2d, 6 weeks of nicotine treatment and 1 or 2 d of withdrawal; %Decrease, difference between 6wk/1,2d and the mean of the two baselines; 8wk/7d, 8 weeks of nicotine treatment and 7 d of withdrawal; %Increase, difference between 8wk/7d and the mean of the two baselines.

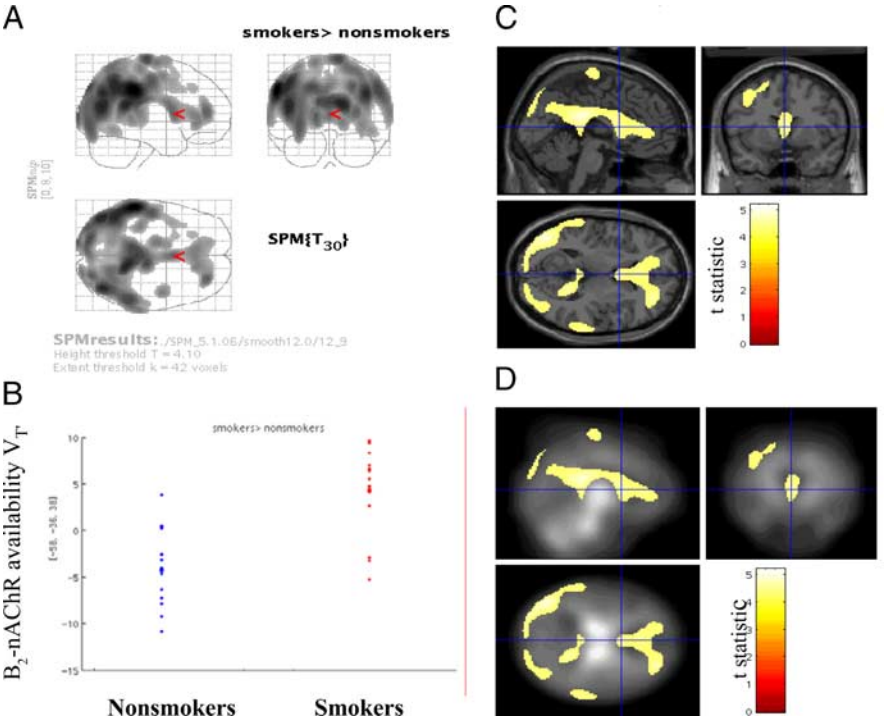

Figure 2. Voxel-based analysis using statistical parametric mapping (SPM2). ***A***, This *t* test demonstrated higher [^{123}I]5-IA uptake in recently abstinent smokers compared with nonsmokers. The *t* statistic map (t_{30} height threshold, $t = 4.10$; extent threshold, $k = 42$ voxels) illustrates brain regions with higher [^{123}I]5-IA regional distribution volume in smokers compared with nonsmokers. ***B***, Scatter plot illustrates the regional distribution volume (V_T') centered around the mean of the voxel with the highest *T* statistic for nonsmokers and smokers. ***C***, The regional localization of significant clusters on a representative MRI from a single subject. ***D***, The regional localization of significant clusters on a representative [^{123}I]5-IA regional distribution volume map from a single subject.

Table 2. β_2*-nAChR availability in nonsmokers versus smokers

Region	Nonsmokers ($n = 16$), mean ± SD	Smokers ($n = 16$), mean ± SD	% Difference smokers vs nonsmokers	*F* statistic	*p* value
Thalamus	48.1 ± 8.4	52.3 ± 8.3	8.7%	2.03	0.1651
Striatum	24.5 ± 3.8	31.1 ± 5.0	26.9%	17.43	0.0002*
Parietal cortex	17.9 ± 2.6	22.9 ± 4.4	27.9%	15.23	0.0005*
Frontal cortex	19.9 ± 2.8	25.1 ± 4.9	26.1%	13.34	0.0010*
Anterior cingulate	18.8 ± 2.7	25.5 ± 4.5	35.6%	26.34	0.00002*
Temporal cortex	20.6 ± 3.4	26.2 ± 4.0	27.2%	18.32	0.0002*
Occipital cortex	18.6 ± 2.8	25.3 ± 4.7	36.0%	23.75	0.00003*
Cerebellum	23.0 ± 4.5	28.8 ± 4.8	25.2%	12.56	0.0013*

β_2*-nAChR availability is reported as V_T' = regional [^{123}I]5-IA activity/total plasma [^{123}I]5-IA activity. *p values <0.00625 are significant after Bonferroni's correction.

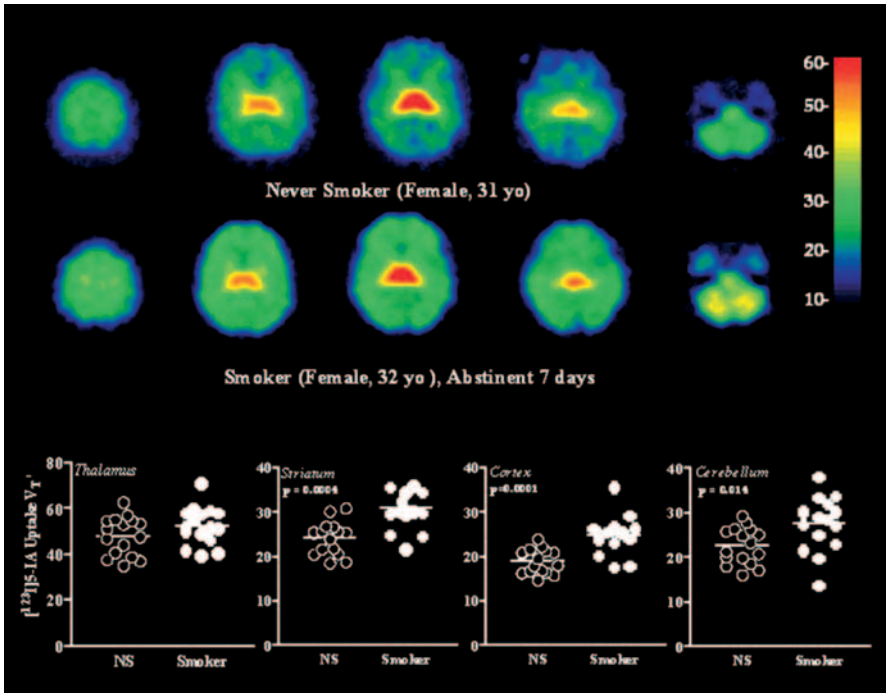

Figure 3. Parametric image of β_2-nAChR availability in a nonsmoker and a smoker and scatter plots illustrating individual regional V_T' values, in nonsmokers ($n = 16$) and smokers ($n = 16$). The parametric images illustrate β_2-nAChR availability at similar transaxial levels of brain, showing frontal, parietal, anterior cingulate, temporal and occipital cortices, and the thalamus and cerebellum in a representative nonsmoker and age- and sex-matched smoker. The color scale is shown with red, yellow, green, and blue corresponding to V_T' values. The scatter plots on the bottom row illustrate individual V_T' values for nonsmokers ($n = 16$) and age- and sex-matched smokers ($n = 16$) in the striatum (mean of caudate and putamen), cortex (mean of all cortical regions including parietal, frontal, anterior cingulate, temporoinsular, and occipital cortices), and the cerebellum. Note that striatal, cortical, and cerebellar [^{123}I]5-IA uptake values were significantly higher in the smokers compared with the nonsmokers (p values = 0.0002, 0.0001, and 0.0013, respectively), whereas there was no significant difference in thalamic [^{123}I]5-IA uptake.

difference), striatum (27% difference), and cerebellum (25% difference) but not in the thalamus (Table 2; Fig. 3).

The relationship between β_2*-nAChR availability and various correlates of smoking behavior was also studied. The voxel-based analyses demonstrated that β_2*-nAChR availability in the anterior cingulate cortex and frontal cortex (BA 5 and BA 6) correlated significantly with the number of days since last cigarette, suggesting that β_2*-nAChR availability increased progressively with continued days of abstinence. We also observed a significant negative correlation between β_2*-nAChR availability in the postcentral gyrus or somatosensory cortex (BA 43) and the urge to smoke to relieve withdrawal symptoms (Table 3). There were no significant correlations between regional β_2*-nAChR availability and number of cigarettes smoked per day, severity of nicotine dependence, severity of nicotine withdrawal, or the urge to smoke for either region of interest analyses or voxel-based analyses.

Discussion

This report provides the first direct evidence that brain β_2*-nAChR densities are higher in the striatum, cerebellum, and cerebral cortex during early abstinence in living human smokers compared with nonsmokers and that β_2*-nAChR availability in the somatosensory cortex correlated with the urge to smoke to relieve withdrawal symptoms. We also observed that β_2*-nAChR availability in the frontal and cingulate cortex correlated positively with the days since last cigarette, suggesting that nicotine has not yet completely cleared from the binding site. These findings were substantiated by our experiment in nonhuman primates that confirmed that higher β_2*-nAChR availability is attributable to nicotine (vs other chemicals in tobacco smoke) and also provided the first evidence that clearance of nicotine or a pharmacologically active metabolite (a metabolite that is occupying the receptor and blocking the radioligand from binding) takes several days after the last administration to clear brain.

The apparent long residence time of nicotine on β_2*-nAChR in brain is surprising given that the terminal half-life of nicotine is 1.6 h in macaques (Schoedel et al., 2003) and that radiolabeled nicotine rapidly clears from brain (Crooks and Dwoskin, 1997; Crooks et al., 1997). The rapid pharmacokinetics were observed, however, after a single administration of a trace dose of intravenous nicotine, and the accumulation of nicotine and/or metabolites (Vainio and Tuominen, 2001) in brain may differ with protracted and repeated nicotine administration. Nicotine is highly lipophilic and, when radiolabeled, demonstrates very high levels of nonspecific brain uptake (Broussolle et al., 1989; Muzic et al., 1998). Therefore, nicotine and/or its metabolites may accumulate in nonspecific compartments in brain, such as white matter, and then diffuse slowly into the gray matter areas in which there are higher levels of nAChRs. Urinary cotinine, the primary metabolite of nicotine, has a longer half-life than nicotine and appears to be a useful indicator of the clearance of nicotine or a metabolite from brain. Importantly, large individual differences in urinary cotinine clearance have been observed in human smokers over the first week of abstinence, with cotinine levels declining to levels comparable with those in nonsmokers over a 4–7 d period after smoking cessation. Interindividual variability in nicotine metabolism in human smokers is expected because individuals with different CYP2A6 genotypes differentially metabolize nicotine (Tyndale and Sellers, 2001).

We did not observe a relationship between β_2*-nAChR availability in brain and the number of cigarettes smoked per day,

Table 3. Relationships between β_2*-nAChR Availability (V_T') and correlates of smoking behavior

Clinical correlate	Brain region	Most significant voxel (*x,y,x*)	Cluster size (K_e)	*T* statistic	Correlation coefficient (*r*)	*p* value uncorrected	*p* value corrected
+ Days since last cigarette	Anterior cingulate	14,12,24	405	8.62	0.95	0.004	0.020
	Frontal cortex BA 6	−20,4,62	269	8.27	0.95	0.014	0.074
	Frontal cortex Paracentral Lobule BA5	40,−44,8	255	7.06	0.93	0.016	0.086
−Smoke to relieve withdrawal	Parietal cortex Postcentral Gyrus BA43	−58,−16,20	311	7.18	0.93	0.016	0.071

unlike a previous study that demonstrated a positive correlation between [^{3}H]nicotine binding to nAChRs on polymorphonuclear lymphocytes and the number of cigarettes smoked per day (Benhammou et al., 2000). This discrepancy may be attributable to differences in nAChR subtypes between tissues or differences between samples from current smokers versus recently abstinent smokers; alternatively, the relationship may have been masked by residual nicotine and/or metabolites in heavy smokers or smokers that were imaged at 4–5 d of abstinence versus 7–9 d when nicotine was more likely to have cleared.

There were notable regional differences in β_2*-nAChR availability in smokers with robustly higher levels throughout the cerebral cortex, striatum, and cerebellum but not thalamus compared with the nicotine-treated nonhuman primates, which exhibited higher [^{123}I]5-IA binding throughout all brain regions. Although a species difference cannot be ruled out, this divergence may suggest that the ability of nicotine to regulate β_2*-nAChR availability is age or sex dependent because the nonhuman primates were male adolescents and the smokers were male and female adults (Slotkin, 2002; Nguyen et al., 2003). The lack of a significant effect on thalamic β_2*-nAChRs in adulthood compared with adolescence, when >90% of smokers start smoking, suggests that it may be of interest to explore the possibility that thalamic β_2*-nAChRs play a role in the initiation of tobacco smoking behavior, whereas β_2*-nAChR adaptations in the striatal reward centers and cortical brain areas contribute both to initiation and maintenance of smoking behavior.

Higher brain [^{123}I]5-IA uptake in recently abstinent smokers suggests greater availability of nicotine binding sites on β_2*-nAChRs. Although β_2 subunits exist in several different combinations with α_2, α_3, α_4, and α_6 subunits, the $\alpha_4\beta_2$ combination is most prevalent and also the most sensitive to upregulation by nicotine (Nguyen et al., 2003; Sallette et al., 2004). Greater β_2*-nAChR availability is not associated with changes in β_2*-nAChR mRNA (Marks et al., 1992; Peng et al., 1994; Zhang et al., 1994) protein synthesis (Buisson and Bertrand, 2001), rate of receptor internalization, postendocytic trafficking, or lysosomal degradation (Darsow et al., 2005), but instead appears to be attributable to occupancy of the nicotine binding site that bridges the α/β subunit interface of the nAChR in an immature, low-affinity conformation that facilitates glycosylation and maturation of the $\alpha_4\beta_2$ nAChR to a more stable conformation with higher affinity for nicotine (Darsow et al., 2005; Sallette et al., 2005). It has been suggested that, in a normal situation, these immature oligomers are rapidly degraded but, in the presence of nicotine, mature and become stabilized in a high-affinity conformation (Sallette et al., 2005). Alternatively, it has also been suggested that the upregulation occurs as a consequence of increased assembly of α_4 and β_2 subunits in the endoplasmic reticulum (Nashmi et al., 2003), enhanced maturation and transport through the secretory pathway to the cell membrane (Sallette et al., 2005), increased transport to the membrane (Harkness and Millar, 2002), and/or decreased receptor turnover (Peng et al., 1994; Wang et al., 1998).

Functionally, greater β_2*-nAChR availability in tobacco smokers likely represents greater numbers of desensitized and inactivated nAChRs (Wonnacott, 1990; Dani and Heinemann, 1996). However, there are some reports suggesting that increased nicotine binding is sometimes paralleled by increased nAChR function (Buisson and Bertrand, 2001). The relationship between greater β_2*-nAChR availability and nAChR function may vary in a region-dependent manner attributable to different subunit combinations that demonstrate increased agonist binding but differ in the effects on function (Rush et al., 2002).

The clinical significance of higher β_2*-nAChR availability in smokers beyond its role in initiating the reinforcing properties of tobacco smoking is unclear. Because the β_2*-nAChR is the initial site of action of nicotine, adaptive changes during acute abstinence may be associated with nicotine withdrawal symptoms that emerge within hours after the last cigarette and persist for 3–4 weeks (Hughes and Hatsukami, 1986). However, there was no evidence for a significant correlation between β_2*-nAChR availability and the severity of nicotine withdrawal assessed by the MWS on the scan day. The lack of a relationship with the MWS score suggests that adaptive changes in β_2-nAChR availability are not responsible for the overall severity of nicotine withdrawal symptoms measured after 4–9 d of abstinence but does not preclude a more direct relationship with individual features of nicotine withdrawal such as anxiety, depression, poor concentration, irritability, and restlessness. Because of the myriad of symptoms and the wide-ranging actions of nicotine on brain neurochemistry, the severity of nicotine withdrawal is likely determined by the complex interplay between β_2*-nAChRs and other neurochemical systems.

Although most withdrawal symptoms resolve after a few days of abstinence, craving (i.e., the urge to smoke) is a prominent feature of nicotine dependence (Tiffany and Drobes, 1991) and is a primary factor associated with relapse (Killen et al., 1997). We observed no relationship between the desire to smoke a cigarette to enhance positive affect and β_2*-nAChR availability. However, we did observe a significant relationship between β_2-nAChR availability in the sensorimotor cortex (Brodmann's area 43) and the urge to smoke to relieve withdrawal symptoms. Thus, if there are fewer β_2-nAChRs in the sensorimotor cortex, there is a greater urge to smoke to relieve withdrawal symptoms. Given that the sensorimotor cortex is involved in mouth and taste reception, these findings may suggest that occupancy of β_2-nAChR by nicotine in the sensorimotor cortex may contribute to some of the sensory cues or "tasting of cigarettes" that has been shown to

play an important role in the relief of craving and the urge to smoke (Rose and Behm, 1994).

In conclusion, these findings provide the first demonstration that recently abstinent smokers have more cortical, striatal, and cerebellar β_2*-nAChR sites available for binding than nonsmokers and that β_2*-nAChRs in the somatosensory cortex contribute to the urge to smoke to relieve withdrawal. Our parallel studies in nonhuman primates were critical in determining the optimal time for human imaging, because time points earlier than 1 week of abstinence, when nicotine or its metabolite were not completely cleared from the brain, might have suggested incorrectly that there was no alteration in β_2*-nAChR availability. Importantly, these studies demonstrate that, when smokers quit smoking, they do so in the face of a significant increase in the receptors normally activated by nicotine. β_2*-nAChR availability during early abstinence likely plays an important role in the ability of smokers to stay abstinent. The findings from these studies are the foundation for future studies that will determine how the higher number of β_2*-nAChRs is normalized by medication or exacerbated in patients who have more difficulty quitting smoking, such as those with neuropsychiatric disorders.

References

Benhammou K, Lee M, Strook M, Sullivan B, Logel J, Raschen K, Gotti C, Leonard S (2000) [^{3}H]Nicotine binding in peripheral blood cells of smokers increase the density of (−)[^{3}H]nicotine binding sites in human brain. Neuropharmacology 39:2818–2829.

Benwell M, Balfour D, Anderson J (1988) Evidence that tobacco smoking increases the density of (−)-[^{3}H]nicotine binding site in human brain. J Neurochem 50:1243–1247.

Breese C, Marks M, Logel J, Adams C, Sullivan B, Collins A, Leonard S (1997) Effect of smoking history on [^{3}H]nicotine binding in human postmortem brain. J Pharmacol Exp Ther 282:7–13.

Broussolle EP, Wong DF, Fanelli RJ, London ED (1989) In *vivo* specific binding of [^{3}H]*l*-nicotine in the mouse brain. Life Sci 44:1123–1132.

Buisson B, Bertrand D (2001) Chronic exposure to nicotine upregulates the human $\alpha4\beta2$ nicotinic acetylcholine receptor function. J Neurosci 21:1819–1829.

Crooks P, Dwoskin L (1997) Contribution of CNS nicotine metabolites to the neuropharmacological effects of nicotine and tobacco smoking. Biochem Pharmacol 54:743–753.

Crooks P, Li M, Dwoskin L (1997) Metabolites of nicotine in rat brain after peripheral nicotine administration: cotinine, nornicotine, and norcotinine. Drug Metab Dispos 25:47–54.

Dani J, Heinemann S (1996) Molecular and cellular aspects of nicotine abuse. Neuron 16:905–908.

Darsow T, Booker T, Pina-Crespo J, Heinemann S (2005) Exocytotic trafficking is required for nicotine-induced up-regulation of $\alpha_4\beta_2$ nicotinic acetylcholine receptors. J Biol Chem 280:18311–18320.

Esterlis I, Krishnan-Sarin S, Staley J (2006) Neurochemical substrates of habitual tobacco smoking. In: Drug abuse handbook, Ed 2 (Karch SB, ed). New York: CRC.

Grant B, Hasin D, Chou P, Stinson F, Dawson D (2004) Nicotine dependence and psychiatric disorders in the United States. Arch Gen Psychiatry 61:1107–1115.

Hariharan M, VanNoord TJFG (1988) A high performance liquid chromataographic method for routine simultaneous determination of nicotine and cotinine in plasma. Clin Chem 34:724–729.

Harkness P, Millar N (2002) Changes in conformation and subcellular distribution of $\alpha4\beta2$ nicotinic acetylcholine receptors revealed by chronic nicotine treatment and expression of subunit chimeras. J Neurosci 22:10172–10181.

Hatsukami D, Hughes J, Pickens R, Svikis D (1984) Tobacco withdrawal symptoms: an experimental analysis. Psychopharmacology 84:231–236.

Heatherton T, Kozlowski L, Frecker R, Fagerstrom K (1991) The Fagerstrom test for nicotine dependence: a revision of the Fagerstrom tolerance questionnaire. Br J Addict 86:1119–1127.

Horti A, Koren A, Lee K, Muhkin A, Vaupel D, Kimes A, Stratton M, London E (1999) Radiosynthesis and preliminary evaluation of 5-[123/125I]iodo-3-(2(*S*)-azetidinylmethoxy)pyridine: a radioligand for nicotinic acetylcholine receptors. Nucl Med Biol 26:175–182.

Hughes J, Hatsukami D (1986) Signs and symptoms of tobacco withdrawal. Arch Gen Psychiatry 43:289–294.

Killen J, Robinson T, Haydel K, Wilson D, Hammer L, Litt I, Taylor C (1997) Prospective study of risk factors for the initiation of cigarette smoking. J Consult Clin Psychol 65:1011–1016.

Lancaster J, Summerlin J, Rainey L, Freitas C, Fox P (1997) The Talairach Daemon, a database server for Talairach atlas labels. NeuroImage 5:S633.

Lancaster J, Woldorff M, Parsons L, Liotti M, Freitas C, Rainey L, Kochunov P, Nickerson D, Mikiten S, Fox P (2000) Automated Talairach atlas for functional brain mapping. Hum Brain Mapp 10:120–131.

Marks M, Burch J, Collins A (1983) Effects of chronic nicotine infusion on tolerance development and cholinergic receptors. J Pharmacol Exp Ther 226:817–825.

Marks M, Stitzel J, Collins A (1985) Time course study of the effects of chronic nicotine infusion on drug response and brain receptors. J Pharmacol Exp Therap 235:619–628.

Marks M, Pauly J, Gross S, Deneris E, Hermans-Borgmeyer I, Heinemann S, Collins A (1992) Nicotine binding and nicotinic receptor subunit RNA after chronic nicotine treatment. J Neurosci 12:2765–2784.

Mukhin A, Gundisch D, Horti A, Koren A, Tamagnan G, Kimes A, Chambers J, Vaupel D, King S, Picciotto M, Innis R, London E (2000) 5-Iodo-A-85380, an $\alpha_4\beta_2$ subtype-selective ligand for nicotinic acetylcholine receptors. Mol Pharmacol 57:642–649.

Musachio JL, Scheffel U, Finley PA, Zhan Y, Mochizuki T, Wagner Jr HN, Dannals RF (1998) 5-[I-123/125]ioo-3-(2(*S*)-azetidinylmethoxy)pyridine, a radioiodinated analog of A-85380 for in vivo studies of central nicotinic acetylcholine receptors. Life Sci 62:351–357.

Musachio JL, Villemagne VL, Scheffel UA, Dannals RF, Dogan AS, Yokoi F, Wong DF (1999) Synthesis of an I-123 analog of A-85380 and preliminary SPECT imaging of nicotinic receptors in baboon. Nucl Med Biol 26:201–207.

Muzic R, Berridge M, Friedland R, Zhu N, Nelson A (1998) PET quantification of specific binding of carbon-11-nicotine in human brain. J Nucl Med 39:2048–2054.

Nashmi R, Dickinson M, Jareg SM, Labarca C, Fraser S, Lester H (2003) Assembly of $\alpha_4\beta_2$ nicotinic acetylcholine receptors assessed with functional fluorescently labeled subunits: effects of localization, trafficking, and nicotine-induced upregulation in clonal mammalian cells and in cultured midbrain neurons. J Neurosci 23:11554–11567.

Nguyen H, Rasmussen B, Perry D (2003) Subtype-selective upregulation by chronic nicotine of high affinity nicotinic receptors in rat brain demonstrated by receptor autoradiography. J Pharmacol Exp Ther 307:1090–1097.

Peng X, Gerzanich V, Anand R, Whiting P, Lindstrom J (1994) Nicotine-induced increase in neuronal nicotinic receptor results from a decrease in the rate of receptor turnover. Mol Pharmacol 46:523–530.

Perry D, Dávila-García M, Stockmeier C, Kellar K (1999) Increased nicotinic receptors in brains from smokers: membrane binding and autoradiography studies. J Pharmacol Exp Ther 289:1545–1552.

Picciotto M, Zoli M, Rimondin R, Lena C, Marubio L, Pich E, Fuxe K, Changeux J (1998) Acetylcholine receptors containing the $\beta2$ subunit are involved in the reinforcing properties of nicotine. Nature 391:173–177.

Pietila K, Lahde T, Attila M, Ahtee L, Nordberg A (1998) Regulation of nicotinic receptors in the brain of mice withdrawn from chronic oral nicotine treatment. Naunyn Schmiedeberg Arch Pharmacol 357:176–182.

Rajeevan N, Zubal I, Rambsy S, Zoghbi S, Seibyl J, Innis R (1998) Significance of nonuniform attenuation correction in quantitative brain SPECT imaging. J Nucl Med 39:1719–1726.

Roll J, Higgins S, Badger G (1996) An experimental comparison of three different schedules of reinforcement of drug abstinence using cigarette smoking as an exemplar. J Appl Behav Anal 29:495–504.

Rose J, Behm F (1994) Inhalation of vapor from black pepper extract reduces smoking withdrawal symptoms. Drug Alcohol Depend 34:225–229.

Rousson V, Gasser T, Seifert B (2002) Assessing intrarater, interrater, and test-retest reliability of continuous measurements. Statist Med 21:3431–3446.

Rush R, Kuryatov A, Nelwon M, Lindstrom J (2002) First and second transmembrane segments of $\alpha3$, $\alpha4$, $\beta2$ and $\beta4$ nicotinic acetylcholine receptor

subunits influence the efficacy and potency of nicotine. Mol Pharmacol 61:1416–1422.

Sallette J, Bohler S, Benoit P, Soudant M, Pons S, Novere NL, Changeux J-P, Corringer P (2004) An extracellular protein microdomain controls upregulation of neuronal nicotinic acetylcholine receptors by nicotine. J Biol Chem 279:18767–18775.

Sallette J, Pons S, Devillers-Thiery A, Soudant M, Prado de Carvalho L, Changeux J-P, Corringer P (2005) Nicotine upregulates its own receptors through enhanced intracellular maturation. Neuron 46:595–607.

Schoedel K, Sellers E, Palmour R, Tyndale R (2003) Down-regulation of hepatic nicotine metabolism and a CYP2A6-like enzyme in African green monkeys after long-term nicotine administration. Mol Pharmacol 63:96–104.

Schwartz R, Kellar K (1983) Nicotinic cholinergic receptor binding sites in the brain: regulation in vivo. Science 220:214–216.

Slotkin T (2002) Nicotine and the adolescent brain: insights from an animal model. Neurotoxicol Teratol 24:369–384.

Staley J, Tamagnan G, Baldwin R, Fujita M, Tikriti MA, Eshima L, Thornback J, Roe D, Lu L, Seibyl J, Innis R (2000) SPECT imaging with the D_4 receptor antagonist L-750,667 in nonhuman primate brain. Nucl Med Biol 27:547–556.

Staley J, van Dyck C, Weinzimmer D, Brenner E, Baldwin R, Tamagnan G, Riccardi P, Mitsis E, Seibyl J (2005) Iodine-123-5-IA-85380 SPECT measurement of nicotinic acetylcholine receptors in human brain by the constant infusion paradigm: feasibility and reproducibility. J Nucl Med 46:1466–1472.

Stitzer M, Bigelow G (1985) Contingent reinforcement for reduced breath carbon monoxide levels: target-specific effects on cigarette smoking. Addict Behav 10:345–349.

Stitzer M, Rand C, Bigelow G, Mead A (1986) Contingent payment procedures for smoking reduction and cessation. J App Behav Anal 19:197–202.

Tiffany S, Drobes D (1991) The development and initial validation of a questionnaire on smoking urges. Br J Addict 86:1467–1476.

Tyndale R, Sellers E (2001) Variable CYP2A6-mediated nicotine metabolism alters smoking behavior and risk. Drug Metab Dispos 29:548–552.

Vainio P, Tuominen R (2001) Cotinine binding to nicotinic acetylcholine receptors in bovine chromaffin cell and rat brain membranes. Nicotine Tob Res 3:177–182.

Wang F, Nelson M, Kuryatov A, Olale F, Cooper J, Keyser K, Lindstrom J (1998) Chronic nicotine treatment upregulates human $\alpha3\beta2$ but not $\alpha3\beta4$ acetylcholine receptors stably transfected in human embryonic kidney cells. J Biol Chem 1998:28721–28732.

Wonnacott S (1990) The paradox of nicotinic acetylcholine receptor upregulation by nicotine. Trends Pharmacol Sci 11:216–219.

Zhang X, Gong Z-H, Hellstrom-Lindahl E, Nordberg A (1994) Regulation of $\alpha4\beta2$ nicotinic acetylcholine receptors in M10 cells following treatment with nicotinic agents. NeuroReport 6:313–317.

Zoghbi S, Tamagnan G, Fujita M, Baldwin RM, Amici L, Tikriti MA, Seibyl J, Innis R (2001) Measurement of plasma metabolites of (*S*)-5-[123I]iodo-3-(2-azetidinylmethoxy)pyridine (5-IA-85380), a nicotinic acetylcholine receptor imaging agent, in nonhuman primates. Nucl Med Biol 28:91–96.